

Spin Flip Diffusion Length and Giant Magnetoresistance at Low Temperatures

Q. Yang, P. Holody, S.-F. Lee, L. L. Henry, R. Loloee, P. A. Schroeder, W. P. Pratt, Jr., and J. Bass

Department of Physics and Astronomy and Center for Fundamental Materials Research,

Michigan State University, East Lansing, Michigan 48824-1116

(Received 28 January 1994)

Measurements at 4.2 K of the magnetoresistance of Co/AgMn, Co/CuMn, Co/AgPt, and Co/CuPt multilayers with the current perpendicular to the layer planes (CPP-MR) show effects of reduced spin diffusion lengths due to alloying of the nonmagnetic metal with impurities that produce spin-spin (Mn) or spin-orbit (Pt) scattering. Combining the data with a theory by Valet and Fert gives the spin diffusion lengths in the alloys.

PACS numbers: 75.50.Rr, 72.10.Fk, 72.15.Gd

Giant magnetoresistance (GMR) in multilayers of alternating ferromagnetic (FM) and nonmagnetic (NM) layers has both scientific and technological interest [1,2]. From its discovery [3], GMR has been described by a two-current model in which independently propagating spin up and spin down electrons undergo spin-dependent scattering in the FM metal and at FM/NM interfaces [3–6]. This scattering causes the multilayer resistance to decrease as the magnetizations of neighboring FM layers rotate from an antiferromagnetic (af) alignment at a low magnetic field H , to a ferromagnetic (fm) one above a saturation field, H_s . At low temperatures, this model [3–6] (and other GMR models [4,7]) contains only two fundamental lengths, the (elastic) mean free path for momentum relaxation, λ_{el} , and the spin diffusion length, l_{sf} . Effects of changes in λ_{el} on GMR are well studied and reasonably well understood [4–6]. Effects of changes in l_{sf} , in contrast, have not been studied at all, except for a partial presentation of the present results [8]. In this Letter, we isolate effects on GMR of reducing the spin diffusion length in the NM metal, l_{sf}^{NM} .

At low temperatures, where electron-magnon scattering is negligible, the usual MR measured with current

flow in the layer planes (CIP-MR) depends only on λ_{el}^{NM} and λ_{el}^{FM} —i.e., neither l_{sf}^{NM} nor l_{sf}^{FM} plays a role. In contrast, when $l_{sf} \gg [\lambda_{el}^{NM}, \lambda_{el}^{FM}]$, l_{sf} is the only fundamental length in the alternative MR measured with current flow perpendicular to the layer planes (CPP-MR) [6,9]. That is, the CPP-MR depends upon λ_{el}^{NM} and λ_{el}^{FM} only indirectly through the resistivities ρ_{FM} and ρ_{NM} . In the more restrictive limit $l_{sf} \gg [\lambda_{el}, t_{FM}, t_{NM}]$ (t_{FM} and t_{NM} = FM and NM metal layer thicknesses), we derived a measurable function for the CPP-MR that is also completely independent of ρ_{NM} and we showed that data for Co/Ag and Co/AgSn multilayers displayed universal behavior when plotted in the form of this function [10]. Valet and Fert (VF) have shown how to analyze deviations from this universal behavior when l_{sf}^{NM} is finite, and thereby how to derive values of l_{sf}^{NM} [9,11]. We will compare our derived values with independent estimates in Table I.

To define the function of interest, we focus upon the quantity we measure, AR_T [the area of the sample ($A \approx 1.2 \text{ mm}^2$) times the total CPP resistance, R_T [12,13]], in two limits, when the magnetizations of neighboring FM layers are oriented ferromagnetically,

TABLE I. Estimated and measured parameters for Co/Ag, Co/AgSn, Co/AgMn, Co/AgPt, Co/Cu, Co/CuMn, and Co/CuPt.

Metal or alloy ^a	Ag	AgSn (4%)	AgMn (6%)	AgMn (9%)	AgPt (6%)	Cu	CuMn (7%)	CuPt (6%)
ρ_{NM}^b (n Ω m) ^b	...	190	100	150	90	...	310	120
ρ_{FM}^c (n Ω m) ^c	9 ± 1	200 ± 20	110 ± 25	155 ± 20	110 ± 20	6 ± 1	270 ± 30	130 ± 10
λ_{el}^{NM} (nm) ^d	85	4.4	8	5.6	9	110	2.1	5.5
λ_{sf}^{NM} (nm) ^e	≈ 17000	≈ 950	≈ 120	≈ 90	≈ 32	≈ 11000	$\approx 24(6)$	≈ 50
l_{sf}^{NM} (nm) ^f	≈ 500	≈ 26	≈ 12	≈ 9	≈ 7	≈ 450	$\approx 3(1.5)$	≈ 7
l_{sf}^{NM} (exp) (nm)			≈ 11	≈ 7	≈ 10		≈ 2.8	≈ 8

^aImpurity concentrations are in atomic %.

^bCalculated from intended impurity concentrations and known resistivities per atomic percent impurity [26].

^cMeasured on sputtered 300–500 nm thick films.

^dCalculated from ρ_{NM} (ρ_{FM} for Ag and Cu) and free-electron equations [27].

^e λ_{sf}^{NM} for CuPt and AgPt was calculated from a free-electron conversion of ESR cross sections [21,22]. The AgMn and CuMn estimates were made by Fert [28] from available information about exchange coupling in these alloys. The CuMn value in parentheses was calculated from a cross section measured from weak localization by Starr, Nishida, and Schultz [24]. The AgSn value assumes a cross section $(3/4)^2$ of that for AgSb in Ref. [21] of Ref. [21]. The sputtered Ag and Cu values assume defect contents $\approx 1\%$ and spin-orbit cross sections $\approx 1 \times 10^{-18} \text{ cm}^2$.

^f $l_{sf}^{NM} = \sqrt{(\lambda_{sf}^{NM} \lambda_{el}^{NM})/6}$ (Ref. [9]).

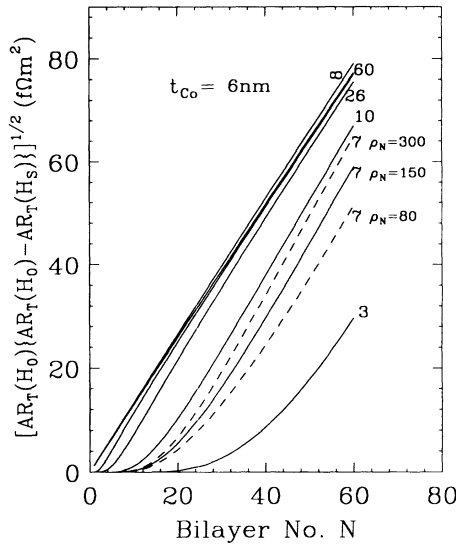


FIG. 1. $\sqrt{AR_T(H_0)[AR_T(H_0) - AR_T(H_S)]}$ vs bilayer number N calculated from VF equations in Ref. [11]. The line labeled ∞ is a fit with parameters for Co/Ag. The solid curves for the indicated values of l_{sf}^{NM} are calculated with these same parameters and $\rho_{NM} = 150$ n Ω m. The dashed curves for $l_{sf}^{NM} = 7$ nm show the effect of varying ρ_{NM} from 80 to 300 n Ω m.

$AR_T^{(fm)}$ —where AR_T is smallest—and when they are ordered antiferromagnetically, $AR_T^{(af)}$ —where AR_T is largest. The physics is in their difference $AR_T^{(af)} - AR_T^{(fm)}$.

In the limit $l_{sf} \gg [\lambda_{el}, t_{FM}, t_{NM}]$, the two current model [12–14] gives a very simple relation upon multiplying $AR_T^{(af)} - AR_T^{(fm)}$ by $AR_T^{(af)}$ and taking the square root [10]:

$$\sqrt{(AR_T^{(af)} - AR_T^{(fm)})AR_T^{(af)}} = N(\beta\rho_{FM}^*t_{FM} + 2\gamma AR_{FM/NM}^*). \quad (1)$$

Here t_{FM} , the number of bilayers N , and the total sample thickness, $t_T = Nt_{FM} + Nt_{NM}$, are set when a sample is made, and ρ_{FM}^* , $R_{FM/NM}^*$, β , and γ are spin-dependent parameters uniquely fixed from measurements on multilayers of given FM and host NM metals [13,15]. The left-hand side (LHS) of Eq. (1) is the function of interest.

For fixed t_{FM} and t_T , a plot of the LHS versus N should give a straight line through the origin, with slope independent of ρ_{NM} . We have shown that Co/Ag and Co/Cu fall on such lines [10,13,16]. If Eq. (1) applies, *data for alloys with a long l_{sf}^{NM} must fall on the same line as the host metal, with no adjustable parameters.* We have shown that this prediction holds for Co/AgSn [10], which provides a strong test of Eq. (1), since AgSn has a $\rho_{NM} \approx 20$ times larger than Ag and also larger than AgMn or AgPt (Table I).

In contrast, for alloys with a short l_{sf}^{NM} (e.g., Mn and Pt), VF predict that a plot of the LHS of Eq. (1) will fall below this line, by an increasing fraction as N decreases

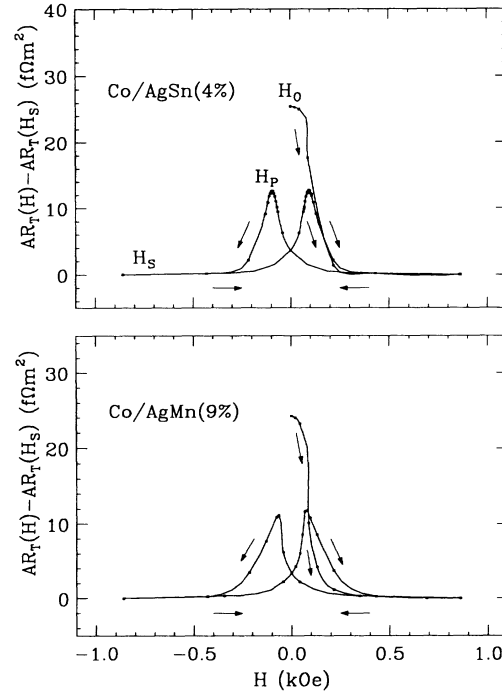


FIG. 2. $AR_T(H) - AR_T(H_S)$ versus H for Co/AgSn(4%) and Co/AgMn(9%) multilayers. The curves are simply guides to the eye.

(t_{NM} increases) [9]. As the VF equations are complex, we show their predictions graphically (Fig. 1) for a range of values of l_{sf}^{NM} , which is the only unknown in the analysis. The line for $l_{sf}^{NM} = \infty$ is simply Eq. (1) for Co/Ag. The curves for reduced l_{sf}^{NM} use the already measured parameters of Eq. (1) for Co/Ag multilayers [10,13,16]. The solid curves are for $\rho_{NM} = 150$ n Ω m, in the middle of our alloy values. The dashed curves for $l_{sf}^{NM} = 7$ nm show that changing ρ_{NM} by a factor of 2 makes only modest changes, but enough that the correct value of ρ_{NM} must be used for each alloy.

Our sample preparation, characterization, and measuring techniques have already been described [13,15]. We limit our analysis to $t_{FM} = 6$ nm and t_T as close to 720 nm as possible, consistent with an integer value of N [10]. Additional data will be published later [17]. To avoid complications of changing magnetic coupling between neighboring Co layers as t_{NM} varies [13,18], we also limit ourselves to $t_{NM} \geq 6$ nm, where any coupling should be weak. To fully test our method of analysis, we apply it to two different NM metals, Ag and Cu, with both a magnetic impurity (Mn) that reduces l_{sf}^{NM} by spin-spin scattering, and a nonmagnetic impurity (Pt) that reduces l_{sf}^{NM} by spin-orbit scattering. We also examine two different concentrations of Mn in Ag.

We measure $AR_T(H)$ at 4.2 K. Figure 2 compares $AR_T(H) - AR_T(H_S)$ for selected Co/AgSn(6 nm/6 nm) and Co/AgMn(6 nm/6 nm) multilayers. The forms and magnitudes are quite similar, suggesting that the magnet-

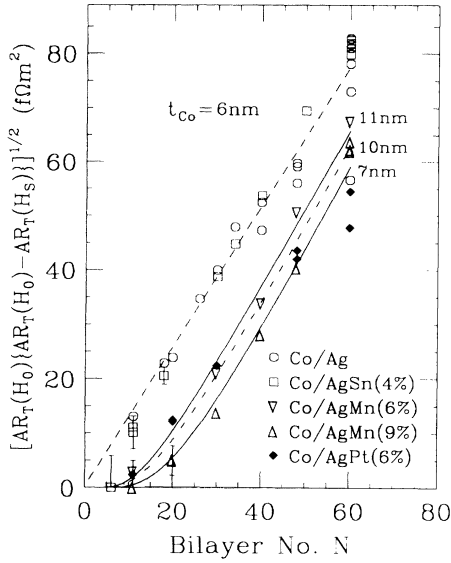


FIG. 3. $\sqrt{AR_T(H_0)[AR_T(H_0) - AR_T(H_s)]}$ vs N for Co/Ag, Co/AgSn(4%), Co/AgMn(6%), Co/AgMn(9%), and Co/AgPt(6%). The dashed line is for $l_{sf}^{NM} = \infty$ [24]. The curves (solid for Co/AgMn and broken for Co/AgPt) correspond to the indicated best fit values of l_{sf}^{NM} . Some measuring uncertainties are also shown. Those not shown are smaller than the symbols or $\leq \pm 5\%$, whichever is larger.

ic impurities do not change the weak interaction between FM layers enough to invalidate our analysis. $AR_T(H)$ is almost always largest in the initially prepared state, which we call H_0 , then decreases until the saturation field H_s is reached, and then cycles through the curves shown, with maxima at the peak field, H_p , which is near the coercive field, H_c .

For $AR_T^{(fm)}$, we take $AR_T(H)$ at $H=1$ kG, the maximum field of our usual measuring system. A higher field system showed that $AR_T(H)$ has reached the desired minimum value by 1 kG for multilayers of all of our metals and alloys except AgMn. For AgMn, $AR_T(H)$ continues to decrease slowly with H above 1 kG, nearly linearly, a behavior not yet understood [17]. Otherwise, the AgMn data look like the rest of our data. As we have not seen similar behavior in CuMn, we presume that this anomaly in AgMn will eventually be found to be irrelevant to our present purpose.

For $AR_T^{(af)}$, we have two choices, $AR_T(H_0)$ and $AR_T(H_p)$. We follow past practice [10,12,13] and use $AR_T(H_0)$, where $AR_T(H)$ is largest, as expected for $AR_T^{(af)}$. This choice is supported by data on Co/Cu multilayers extending from antiferromagnetically coupled samples to uncoupled ones [19]. Our conclusions stay the same if we systematically use $AR_T(H_p)$ instead, and values for l_{sf}^{NM} change by less than 50% [16]. Most of our Co/AgPt and Co/CuPt data, and some recent Co/Cu data, had values of $AR(H_0)$ closer to $AR(H_p)$ than usual. We present these data unmodified, and consider alter-

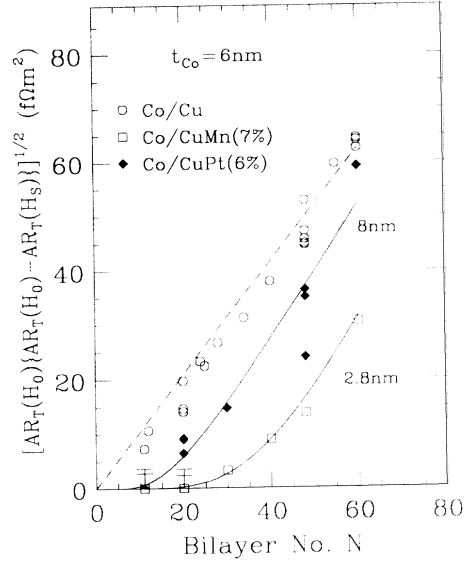


FIG. 4. $\sqrt{AR_T(H_0)[AR_T(H_0) - AR_T(H_s)]}$ vs N for Co/Cu and Co/CuMn(9 at.%). The dashed line and curves, associated values of l_{sf}^{NM} , and measuring uncertainties are as described in Fig. 3.

native analyses elsewhere [16]; these alternatives do not change l_{sf}^{NM} by more than the 50% already noted.

Plots of the LHS of Eq. (1) vs N are shown for our Ag-based data in Fig. 3 and for our Cu-based data in Fig. 4. As noted above, the Co/Ag and Co/Cu data are consistent with the required straight lines passing through the origin [20], and the Co/AgSn data also fall close to the line for Co/Ag.

To analyze the other alloy data, we use the values of ρ_{NM} for our sputtered alloys given in Table I. The VF theory then gives the best fits for l_{sf}^{NM} shown in the figures.

For CuPt [21] and AgPt [22], we can compare our values of l_{sf}^{NM} with ones derived from published ESR values for the spin-flip mean free path, λ_{sf}^{NM} (see Table I). Differences in ESR values among investigators [23] suggest uncertainties in λ_{sf}^{NM} of at least a factor of 2, giving more than a 50% uncertainty in l_{sf}^{NM} . The values of l_{sf}^{NM} for Pt in Table I lie within 50% of ours.

For the other alloys, we use the estimates of l_{sf}^{NM} described in Table I. The value $l_{sf}^{NM} \approx 26$ nm for AgSn is large enough that we cannot distinguish it from $l_{sf}^{NM} \approx \infty$ to within our reproducibility. The estimates for paramagnetic Mn in Ag and Cu may be only lower bounds, since these alloys are in a spin-glass state at 4.2 K—even in layers only 6 nm thick [24]—where coherent interactions between Mn ions could increase l_{sf}^{NM} . Our fits in Fig. 3 agree with the unmodified estimates for AgMn in Table I. The estimate for CuMn is 10% larger than our fit, but a recent measurement is $\approx 50\%$ less [23]. Both lie within our uncertainties.

Some loose threads remain. The VF equations were in-

initially shown to be valid only for $l_{sf} \gg \lambda_{el}$ [9], a criterion not met by our Mn or Pt alloys, for which Table I and Figs. 3 and 4 give $l_{sf}^{NM} \approx \lambda_{el}^{NM}$. Valet [25] has extended the analysis to second order in $\lambda_{el}^{NM}/l_{sf}^{NM}$, and found a correction term $\approx 0.25 l_{sf}^{NM} (\lambda_{el}^{NM}/l_{sf}^{NM})$ [2]. Further analysis must show if such a simple correction holds to all orders. As noted above, the high field negative linear MR in AgMn must also still be understood, and we must clarify the relationship between $R_T^{(af)}$, $R_T(H_0)$, and $R_T(H_p)$.

To summarize, we have used the CPP geometry to provide direct evidence for changes in GMR in magnetic multilayers due to reductions in the spin diffusion length, l_{sf}^{NM} . Our data display the qualitative features predicted by VF and our derived values of l_{sf}^{NM} agree reasonably well with independent estimates.

This work was supported by NSF Grant No. DMR 92-22614, the MSU Center for Fundamental Materials Research, and the Ford Motor Co. We thank A. Fert and T. Valet for helpful assistance under joint U.S.-France Grants No. NSF-INT-92-16909 and No. CNRS-A10693, V. Shull for confirming the impurity concentrations in our alloys by energy dispersive x-ray measurements, and A. F. Starr, A. Nishida, and S. Schultz for letting us quote their CuMn value prior to its publication.

[1] L. Falicov *et al.*, *J. Mater. Res.* **5**, 1299 (1990).

[2] R. E. Camley and R. L. Stamps, *J. Phys. Condens. Matter* **5**, 3727 (1993), and references therein.

[3] M. N. Baibich *et al.*, *Phys. Rev. Lett.* **61**, 2472 (1988).

[4] R. E. Camley and J. Barnas, *Phys. Rev. Lett.* **63**, 664 (1989); P. M. Levy *et al.*, *Phys. Rev. Lett.* **65**, 1643 (1990); S. Zhang *et al.*, *Phys. Rev. B* **45**, 8689 (1992); A. Barthelemy and A. Fert, *Phys. Rev. B* **43**, 13 124 (1991); J.-I. Inoue *et al.*, *J. Phys. Soc. Jpn.* **60**, 376 (1991); D. M. Edwards *et al.*, *J. Magn. Magn. Mater.* **114**, 252 (1992); H. Camblong and P. M. Levy, *Phys. Rev. Lett.* **69**, 2835 (1992); L. Falicov and R. Q. Hood, *J. Magn. Magn. Mater.* **121**, 362 (1993); G. E. W. Bauer, *Phys. Rev. Lett.* **69**, 1676 (1992); A. Vedyayev *et al.*, *Europhys. Lett.* **19**, 329 (1992).

[5] S. Zhang, *Appl. Phys. Lett.* **61**, 1855 (1992); S. Zhang and P. M. Levy, *J. Appl. Phys.* **73**, 5315 (1993).

[6] H. Camblong *et al.*, *Phys. Rev. B* **47**, 4735 (1993); S. Zhang and P. M. Levy, *Phys. Rev. B* **47**, 6776 (1993).

[7] M. B. Stearns, *J. Magn. Magn. Mater.* **104-107**, 1745 (1992); *J. Appl. Phys.* **72**, 5354 (1992); (to be published).

[8] The data for Co/AgMn(9%) and Co/CuMn(7%) in this Letter are given also by J. Bass *et al.*, *J. Appl. Phys.* (to be published).

[9] T. Valet and A. Fert, *J. Magn. Magn. Mater.* **121**, 378 (1993); *Phys. Rev. B* **48**, 7099 (1993).

[10] S.-F. Lee *et al.*, *J. Magn. Magn. Mater.* **118**, L1 (1993).

[11] The VF equations contain two parameters, l_{sf}^{FM} and l_{sf}^{NM} . Since we do not dope the FM metal, we assume that l_{sf}^{FM} is large compared to t_{FM} and does not change as we dope the NM metal. l_{sf}^{NM} is then the only new parameter.

[12] S. F. Lee *et al.*, *Phys. Rev. B* **46**, 548 (1992).

[13] P. A. Schroeder *et al.*, in *Magnetism and Structure in Systems of Reduced Dimension*, NATO ASI, Ser. B, Vol. 309 (Plenum, New York, 1993), p. 129; W. P. Pratt, Jr. *et al.*, *J. Appl. Phys.* **73**, 5326 (1993); W. P. Pratt, Jr. *et al.*, *J. Magn. Magn. Mater.* **126**, 406 (1993).

[14] S. Zhang and P. M. Levy, *J. Appl. Phys.* **69**, 4786 (1991).

[15] W. P. Pratt, Jr. *et al.*, *Phys. Rev. Lett.* **66**, 3060 (1991).

[16] Q. Yang *et al.* (unpublished); P. Holody (unpublished).

[17] It is known that the spin glasses AgMn and CuMn exhibit negative linear MR at high fields [see, e.g., V. M. Beylin *et al.*, *Phys. Met. Metall.* **61**, 68 (1986); A. K. Nigam *et al.*, *J. Appl. Phys.* **50**, 7361 (1979)], but Nb/AgMn/Nb sandwiches do not reproduce the multilayer results.

[18] S. S. P. Parkin *et al.*, *Phys. Rev. Lett.* **64**, 2304 (1990); S. S. P. Parkin *et al.*, *Phys. Rev. Lett.* **66**, 2152 (1991); D. H. Mosca *et al.*, *J. Magn. Magn. Mater.* **94**, L1 (1991).

[19] P. A. Schroeder *et al.*, *Mater. Res. Soc. Symp. Proc.* **313**, 47 (1993).

[20] The dashed lines through the Co/Ag and Co/Cu data are not simply best fits to the data of Figs. 3 and 4, but rather come from global fits to several sets of data with different Co (and Ag) thicknesses (see Refs. [13], [16], and [18]).

[21] P. Monod and S. Schultz, *J. Phys. (Paris)* **43**, 393 (1982).

[22] A. C. Gossard, T. Y. Kometani, and J. H. Wernick, *J. Appl. Phys.* **39**, 849 (1968).

[23] A. F. Starr, A. Nishida, and S. Schultz (unpublished).

[24] J. Bass and J. A. Cowen, in *Recent Progress in Random Magnets*, edited by D. H. Ryan (World Scientific, Singapore, 1992), p. 177.

[25] T. Valet (unpublished).

[26] J. Bass, in *Metals: Electronic Transport Phenomena* Landolt-Bornstein, New Series, Group 3, Vol. 15, Pt. a, edited by K.-H. Hellwege and J. L. Olsen (Springer-Verlag, Berlin, 1982).

[27] N. W. Ashcroft and N. D. Mermin, *Solid State Physics* (W. B. Saunders, Philadelphia, 1976).

[28] A. Fert (unpublished).